


Cardioprotective kinase signaling to subsarcolemmal and interfibrillar mitochondria is mediated by caveolar structures

Wylly Ramsés García-Niño¹ · Francisco Correa¹ · Julia Isabel Rodríguez-Barrena¹ · Juan Carlos León-Contreras² · Mabel Buelna-Chontal¹ · Elizabeth Soria-Castro³ · Rogelio Hernández-Pando² · José Pedraza-Chaverri⁴ · Cecilia Zazueta¹ 

Received: 29 July 2016 / Accepted: 31 January 2017 / Published online: 3 February 2017
© Springer-Verlag Berlin Heidelberg 2017

Abstract The demonstration that caveolin-3 overexpression reduces myocardial ischemia/reperfusion injury and our own finding that multiprotein signaling complexes increase in mitochondria in association with caveolin-3 levels, led us to investigate the contribution of caveolae-driven extracellular signal-regulated kinases 1/2 (ERK1/2) on maintaining the function of cardiac mitochondrial subpopulations from reperfused hearts subjected to postconditioning (PostC). Rat hearts were isolated and subjected to ischemia/reperfusion and to PostC. Enhanced cardiac function, reduced infarct size and preserved ultrastructure of cardiomyocytes were associated with increased formation of caveolar structures, augmented levels of caveolin-3 and mitochondrial ERK1/2 activation in PostC hearts in both subsarcolemmal (SSM) and interfibrillar (IFM) subpopulations. Disruption of caveolae with methyl- β -

cyclodextrin abolished cardioprotection in PostC hearts and diminished pho-ERK1/2 gold-labeling in both mitochondrial subpopulations in correlation with suppression of resistance to permeability transition pore opening. Also, differences between the mitochondrial subpopulations in the setting of PostC were evaluated. Caveolae disruption with methyl- β -cyclodextrin abolished the cardioprotective effect of postconditioning by inhibiting the interaction of ERK1/2 with mitochondria and promoted decline in mitochondrial function. SSM, which are particularly sensitive to reperfusion damage, take advantage of their location in cardiomyocyte boundary and benefit from the cardioprotective signaling driven by caveolae, avoiding injury propagation.

Keywords Cardioprotection · Postconditioning · Mitochondrial subpopulations · Caveolae · Mitochondrial ERK1/2

Electronic supplementary material The online version of this article (doi:10.1007/s00395-017-0607-4) contains supplementary material, which is available to authorized users.

✉ Wylly Ramsés García-Niño
wramsegarcia@gmail.com

✉ Cecilia Zazueta
azazueta@yahoo.com

¹ Departamento de Biomedicina Cardiovascular, Instituto Nacional de Cardiología “Ignacio Chávez”, Juan Badiano No. 1, Sección XVI, 14080 Ciudad de México, México

² Departamento de Patología, Instituto Nacional de Ciencias Médicas y Nutrición “Salvador Zubirán”, 14000 Ciudad de México, México

³ Departamento de Patología, Instituto Nacional de Cardiología “Ignacio Chávez”, 14080 Ciudad de México, México

⁴ Departamento de Biología, Facultad de Química, Universidad Nacional Autónoma de México, 04510 Ciudad de México, México

Introduction

Mitochondrial dysfunction characterized by impaired oxidative phosphorylation, increased generation of reactive oxygen species (ROS), mitochondrial calcium overload and activation of the mitochondrial permeability transition pore (mPTP) is intimately associated with ischemia/reperfusion (I/R) damage [11]. It is well established that cardioprotective strategies including ischemic postconditioning (PostC) diminish I/R injury in both humans and animal models through the activation of several intracellular signaling pathways [22]. Reperfusion injury salvage kinases (RISK), particularly the extracellular signal-regulated kinase 1/2 (ERK1/2), not only contributes to PostC-induced cardioprotection by activating cytosolic downstream targets, but

also by interacting with proteins that reside in diverse subcellular compartments/organelles [41]. This hypothesis is sustained by reports of redox-dependent translocation of phosphorylated ERK1/2 to mitochondria by diazoxide [32] and, of plasmatic membrane signaling microdomains (signalosomes) assembled into caveolae that deliver cytosolic signals to the outer mitochondrial membrane [21, 43]. Furthermore, caveolae-mediated translocation of cardioprotective signals to mitochondria has been established by disrupting cholesterol-rich membrane structures [14, 19, 23, 35, 38].

However, the relationship between caveolae and ERK1/2 signaling with mitochondria has yet to be validated. Therefore, the aim of this study was to evaluate: (1) the possible association of caveolar structures with subsarcolemmal mitochondria (SSM) and with interfibrillar mitochondria (IFM); (2) the presence of ERK1/2 in these structures and (3) the functional response of both subpopulations to cardioprotective signaling.

Materials and methods

This investigation was performed in accordance with the Guide for the Care and Use of Laboratory Animals, published by the United States National Institutes of Health (US-NIH) and approved by the Ethics Committee of the National Institute of Cardiology I. Ch (INC-13806). Experimental work followed the guidelines of the Norma Oficial Mexicana for the use and care of laboratory animals (NOM-062-ZOO-1999) and for the disposal of biological residues (NOM-087-SEMARNAT-SSA1-2002). Reagents, antibodies and buffers composition are included in Supplementary Appendix A.

Experimental design

Male Wistar rats (250–300 g) were anesthetized with a single dose of sodium pentobarbital (60 mg/kg i.p) and complete lack of pain response was assessed by determining pedal withdrawal reflex. The hearts were rapidly excised via midsternal thoracotomy, placed momentarily in ice-cold Krebs–Henseleit buffer and perfused retrogradely via the aorta at a constant flow rate of 12 ml/min with Krebs–Henseleit solution, which was continuously bubbled with 95% O₂ and 5% CO₂ at 37 °C. Cardiac performance was measured at left ventricular end-diastolic pressure (LVEDP) of 10 mmHg using a latex balloon inserted into the left ventricle and connected to a pressure transducer. Throughout the experiment, left ventricular developed pressure (LVDP) was recorded using a computer acquisition data system designed by the Instrumentation and Technical Development Department of the National

Institute of Cardiology (Mexico City, Mexico). Heart rate (HR) expressed as beats/min was obtained from the left ventricular pressure waveform [8]. The double product (DP) was calculated by multiplying HR by LVDP. Hearts were perfused for 20 min to reach a steady state and then subjected to the different protocols. The experimental groups were: (1) P, hearts perfused for additional 90 min (control); (2) I/R, hearts subjected to global ischemia for 30 min by turning off the pumping system and 60 min of reperfusion; (3) PostC, hearts subjected to 30 min of ischemia, to postconditioning (5 cycles of 30 s reperfusion and 30 s ischemia) and to 60 min of reperfusion (Fig. 1a). Additional experiments were performed in the presence of 0.1 mM methyl- β -cyclodextrin (M β CD) to link the formation of caveolae with ERK1/2 driving to mitochondria (Fig. 4a).

Infarct size

Infarct size was measured using triphenyltetrazolium chloride (TTC) staining [5, 20]. Heart was frozen and cut into 3-mm transverse slices. The slices were incubated in 1% TTC solution for 20 min at 37 °C and then immersed in formalin solution for 20 min to enhance the contrast between stained and unstained tissue. TTC stains living tissue into a deep red color. Digital images of heart slices were obtained and analyzed using the ImageJ 1.48 software (NIH, Bethesda, MD, USA). Infarct size was expressed as a percentage and calculated by dividing the area of infarct by total area.

Electron microscopy

At the end of the experiment, ventricular tissue was sectioned into pieces of 1 mm of thickness, fixed by immersion in 2.5% glutaraldehyde for 4 h at 4 °C, post-fixed in 2% OsO₄ buffer, dehydrated with increasing concentrations of ethanol and infiltrated with epoxy resins. Ultrathin sections of 70 nm were contrasted in uranyl acetate and lead citrate to be further examined with an FEI Tecnai transmission electron microscope (Hillsboro, OR, USA). Mitochondrial areas and cristae-integrated density were measured using the Multi Measure ROI tool of ImageJ 1.48 software, from digital images obtained at similar magnifications. Caveolae were identified in both open (structures visibly integrated into the sarcolemma) and closed (vesicles) configurations. Total number of caveolae per membrane length were counted and compared between experimental groups. For immunogold labeling, ventricular tissue was fixed in 4% paraformaldehyde, dehydrated and infiltrated with LR-White hydrosoluble resin. Ultrathin sections of 60–70 nm were placed on nickel grids and incubated

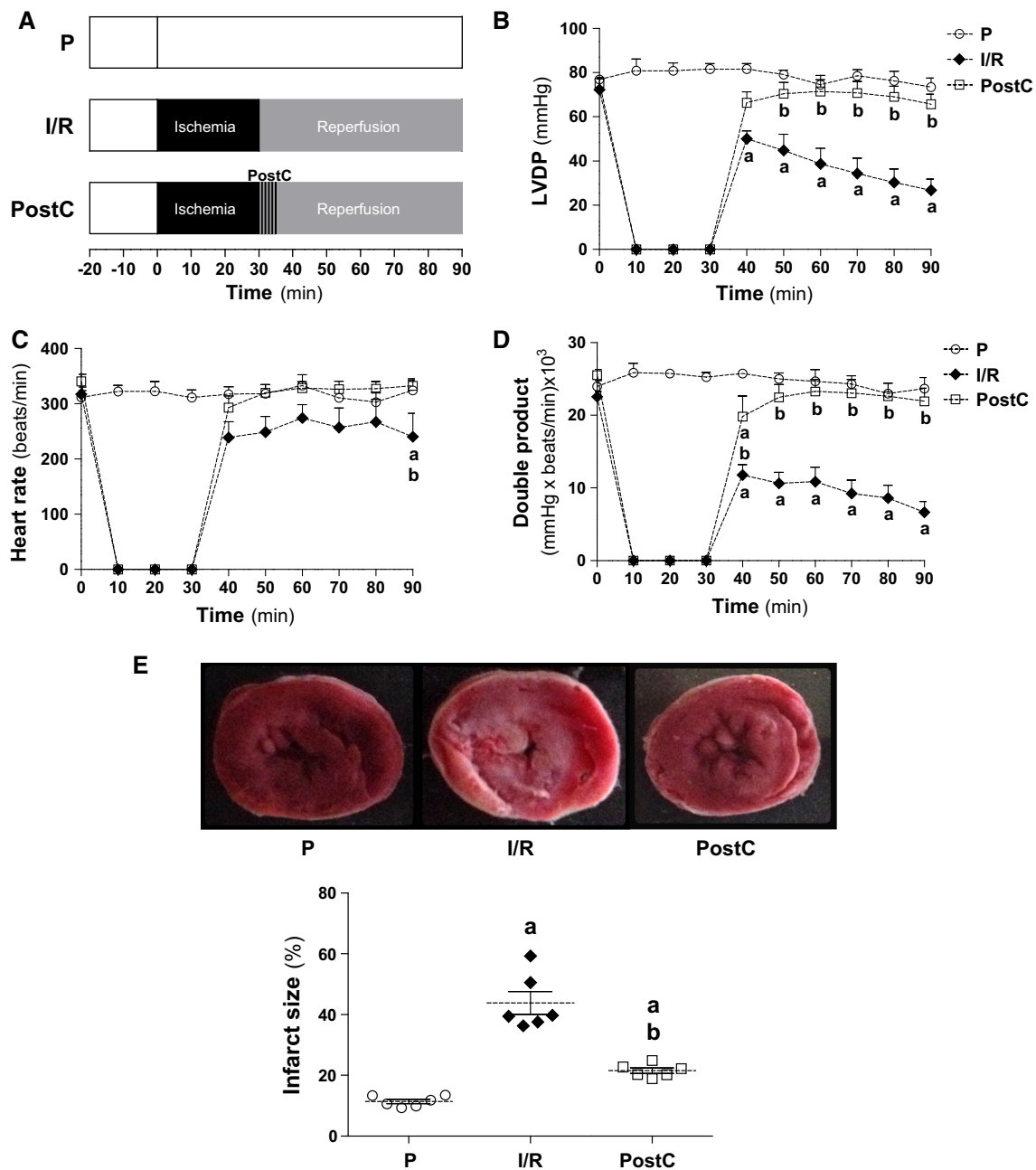


Fig. 1 Cardiac function parameters and myocardial infarct size. **a** Schematic representation of the experimental protocol: perfused hearts (P), ischemic-reperfused hearts (I/R) and postconditioned hearts (PostC). **b** Left ventricular diastolic pressure (LVDP), **c** heart rate and **d** double product. **e** Infarct size percentage and representative

images of TTC-stained hearts. Values are mean \pm SEM, $n = 6-8$. ^a $p < 0.05$ vs. P; ^b $p < 0.05$ vs. I/R (two-way ANOVA). The main effect for group yielded an F ratio of $(2,162) = 71.58$, $p < 0.001$. The main effect for time yielded an F ratio of $(9,162) = 77.84$, $p < 0.001$. The interaction effect was significant; $F(18,162) = 32.49$, $p < 0.001$

overnight at 4 °C with specific anti-caveolin-3 (1:50) or anti-pho-ERK1/2 (1:10) antibodies followed by a 2-h incubation at room temperature with goat anti-mouse IgG conjugated to 12-nm gold particles and goat anti-rabbit IgG conjugated to 5-nm gold particles, respectively. The grids were contrasted with uranyl acetate and lead citrate before transmission electron microscopy examination.

Mitochondrial isolation

Heart tissue was finely minced and washed in cold buffer A. Total mitochondria were obtained according to Chávez et al. [6]; whereas, mitoplasts, outer membrane and proteins from the intermembrane space were isolated as previously reported [10]. SSM and IFM subpopulations were isolated at 4 °C as described [25]. For isolation of SSM,

heart tissue was homogenized in buffer A with five strokes of a Teflon pistil in a glass potter. The homogenate was spun down (750g, 10 min) and the resultant supernatant was centrifuged for 10 min at 12,000g. The pellet was suspended in buffer B supplemented with 1.5% albumin fatty acid-free (FAF), incubated for 10 min on ice and centrifuged (12,000g, 10 min). The pellet was collected and suspended in buffer B. For isolation of IFM, the sediment of the first centrifugation was resuspended in buffer A and after addition of 0.250 mg/ml of the protease nagarse, incubated further during 5 min on ice. Then it was homogenized with five strokes of a Teflon pistil in a glass potter and centrifuged (750g, 10 min), the resultant supernatant was centrifuged for 10 min at 12,000g. This pellet was suspended in buffer B supplemented with 1.5% albumin FAF, incubated for 10 min on ice and centrifuged (12,000g, 10 min). The pellet was collected and suspended in buffer B. Mitochondria were further purified by 60% percoll gradient ultracentrifugation. Protein concentration was determined by the Lowry method [28].

Immunoblot analysis

Connexin 43 (Cx43) and sarcoplasmic reticulum Ca^{2+} -ATPase (SERCA) were measured to assess purity of the differential mitochondrial preparations. SSM and IFM were incubated in Buffer B plus 2.0 mM digitonin for 10 min on ice and pelleted by centrifugation according to Boengler et al. [4]. Mitochondrial protein (100 μg) was analyzed by immunoblotting with anti-Cx43 (1:1000) and with anti-SERCA (1:1000). ANT content was determined as the loading marker (Supplementary Figure S.1).

Caveolin-3 and ERK1/2 content in SSM and IFM mitochondria (100 μg) was analyzed by immunoblotting with anti-caveolin-3 (1:1000); anti-ERK1/2 (1:1000) and anti-pho-ERK1/2 (1:1000). The ratio between phosphorylated protein and total protein was obtained in the same membrane in all experiments and ANT (1:1000) was used as the loading marker.

Cytochrome c (cyt c) release from SSM and IFM was evaluated as described [17]. Briefly, mitochondrial protein (0.7 mg/ml) was incubated in buffer C in the presence of 200 μM ADP, 10 mM malate/10 mM glutamate and 100 μM Ca^{2+} , with or without CsA (1 μM) for 10 min and pelleted by centrifugation. The supernatants were precipitated with trichloroacetic acid and pellets were washed once. Released cyt c in supernatant fractions and retained cyt c in mitochondrial pellets (50 μg) were analyzed by immunoblotting with anti-cyt c (1:3000). ANT was determined as the loading marker. Protein bands were analyzed by densitometry with the Image Studio Lite 4.0.21. software (LI-COR Biosciences).

Mitochondrial permeability transition pore (mPTP) opening

Mitochondrial swelling was assayed spectrophotometrically using a Beckman DU-65 spectrophotometer [13]. Briefly, mitochondria (0.7 mg/ml) were suspended in 1.4 ml of swelling buffer. Changes in absorbance at 540 nm (A540) were followed, after addition of energizing substrates and 100 μM CaCl_2 with or without CsA (1 μM).

Extramitochondrial free Ca^{2+} was monitored using the hexapotassium salt of Calcium Green-5N [1]. Isolated mitochondria (0.25 mg/ml) were suspended in buffer C. Calcium green (60 nM) fluorescence was monitored with excitation at 506 nm and emission at 531 nm in presence of malate/glutamate after the addition of 100 μM CaCl_2 with or without 1 μM CsA. CCCP (0.1 μM) was used to induce Ca^{2+} release from mitochondria. The values were represented as relative fluorescence units (RFU).

Mitochondrial inner membrane potential ($\Delta\Psi_m$) was qualitatively evaluated by measuring changes in Rhodamine 123 fluorescence with excitation at 507 nm and emission at 529 nm, using a Perkin-Elmer luminescence spectrophotometer LS50B [7]. Dye (30 nM) and mitochondria (0.25 mg/ml) were added in buffer C supplemented with 6.4 mM MgCl_2 , 10 mM malate/10 mM glutamate, 1 μM oligomycin, 100 μM CaCl_2 and 0.1 μM CCCP added at different time points in the presence or the absence of CsA (1 μM). The values were represented as RFU.

Mitochondrial oxygen consumption

Mitochondrial oxygen consumption was measured polarographically using a Clark type oxygen electrode (Yellow Springs Instruments, Yellow Springs, OH, USA) [9]. Freshly isolated mitochondria (0.6 mg/ml) were suspended in 1.7 ml of respiration buffer. State 4 respiration was evaluated in the presence of NADH-linked substrates (10 mM glutamate/10 mM malate) or with 10 mM succinate plus 1 μM rotenone. State 3 respiration was stimulated by the addition of 200 μM ADP. Respiratory control (RC) was calculated as the ratio between State 3 and State 4. Uncoupled respiration was measured by adding 0.1 μM CCCP. The ADP/O ratio (phosphorylation efficiency) was calculated from the added amount of ADP and total amount of oxygen consumed during State 3.

Oxidative stress markers and antioxidant enzyme activities

Oxidative stress markers and antioxidant enzyme activities were evaluated using a Synergy HT multimode microplate reader as described [18]. Malondialdehyde (MDA) content was measured by the reaction with 1-methyl-2-

phenylindole at 586 nm, using a standard curve of tetramethoxypropane. Glutathione (GSH) content was evaluated by following the formation of a fluorescent adducts between GSH and monochlorobimane in a reaction catalyzed by GST. A standard curve of GSH was used and the fluorescence measured at excitation and emission wavelengths of 385 and 478 nm, respectively. Aconitase activity was assayed at 240 nm by determining the rate of formation of the intermediate product, *cis*-aconitate, from the interconversion of L-citrate and isocitrate. The extinction coefficient used for *cis*-aconitate was $3.6 \text{ mM}^{-1} \text{ cm}^{-1}$.

Superoxide dismutase (SOD) activity was measured spectrophotometrically at 560 nm by measuring the NBT reduction to formazan. The amount of protein that inhibits NBT reduction to 50% of maximum was defined as one unit of SOD activity. Catalase (CAT) activity was evaluated by monitoring the decomposition of H_2O_2 by CAT contained in the samples at 240 nm. The data were expressed as k per milligram of protein, where k is the first-order reaction rate constant. Glutathione reductase (GR) activity was assayed by using glutathione disulfide (GSSG) as substrate and measuring the disappearance of NADPH at 340 nm. Glutathione peroxidase (GPx) activity was assayed by following NADPH consumption at 340 nm. When GPx reduces H_2O_2 , GSH is oxidized to GSSG that is additionally reduced to GSH by GR using NADPH. One unit of GPx and GR is defined as the amount of enzyme that oxidizes 1 nmol of NADPH per minute.

Statistical analysis

Results were expressed as mean \pm standard error of the mean (SEM). Data were analyzed by one-way ANOVA or two-way ANOVA followed by Bonferroni's multiple-comparisons test using Prism 5.0 software (GraphPad, San Diego, CA, USA). A p value <0.05 was considered statistically significant.

Results

PostC supports cardiac function, reduces infarct size and augments PHO-ERK1/2 levels in mitochondria

LVDP and heart rate were maintained in P hearts during 110 min of constant perfusion, whereas LVDP decreased early and until the end of reperfusion in I/R hearts ($p < 0.05$). PostC hearts recovered LVDP since the first 20 min of reperfusion (Fig. 1b). Heart rate was significantly reduced after 60 min of reperfusion in comparison with P and PostC hearts (Fig. 1c). Accordingly, the DP was significantly lower in I/R hearts than in P and PostC hearts ($p < 0.05$) (Fig. 1d). Infarct size increased to 45% in I/R

hearts as compared with 11 and 22% in P and PostC hearts, respectively ($p < 0.05$) (Fig. 1e). PostC-induced cardioprotection was mimicked by pho-ERK1/2 activation in mitochondria (Supplementary Figure S.2A). To determine the location of ERK1/2 within these organelles, we obtained mitoplasts, the outer membrane fraction and intermembrane space proteins of P, I/R and PostC mitochondria. Pho-ERK1/2 increased in the outer membrane and in the intermembrane space of mitochondria from PostC hearts in comparison with mitochondria from P and I/R hearts; no changes were found in mitoplasts between the three groups (Supplementary Figure S.2B).

PostC increases caveolae-like structures linked with ERK1/2 activation in mitochondrial subpopulations

Caveolae-like structures were observed as flask-shaped invaginations in the sarcolemma and in form of vesicles (closed configuration) in all groups (Fig. 2). Caveolae diminished in the I/R group (Fig. 2b) as compared with control hearts (Fig. 2a) and PostC hearts (Fig. 2c). In this group, such structures were found mainly in its closed configuration (Fig. 2d; $p < 0.05$) near the sarcolemmal membrane making apparent connections with SSM (Fig. 2c) and to minor extent in the interfibrillar area. Accordingly, immunoelectron microscopy (Fig. 2e) and western blot analysis (Fig. 2f) showed higher levels of the essential structural protein caveolin-3 in SSM than in IFM ($p < 0.05$) from PostC hearts. The parallelism found between both studies, supports the interaction between caveolae and SSM. On the other hand, pho-ERK1/2 immunogold labeling revealed increased levels of this kinase in SSM from the PostC group (Fig. 3c) as compared with SSM from the P and I/R groups (Fig. 3a, b). Electron-dense spots corresponding to ERK1/2 activation were also superior in number in the IFM subpopulation of the PostC group (Fig. 3f) than in the P and the I/R (Fig. 3d, e). Magnified ERK1/2 labeling is shown in Supplementary Figure S.3. ERK1/2 activation in SSM from PostC hearts (Fig. 3g) was further corroborated by western blot (Fig. 3h) and correlated with their caveolin-3 content (Fig. 2f). Although it is clear that PostC increased pho-ERK1/2 location in both mitochondrial subpopulations, our reasoning is that the western blot analysis indicates a more realistic pattern of activation, as pho-ERK1/2 was normalized against total ERK1/2 in purified mitochondria.

M β CD abolishes cardioprotection, disrupts caveolae formation and abolish ERK1/2 signaling in PostC hearts

Some PostC hearts were treated with 0.1 mM methyl- β -cyclodextrin (M β CD) for 20 min during the stabilization

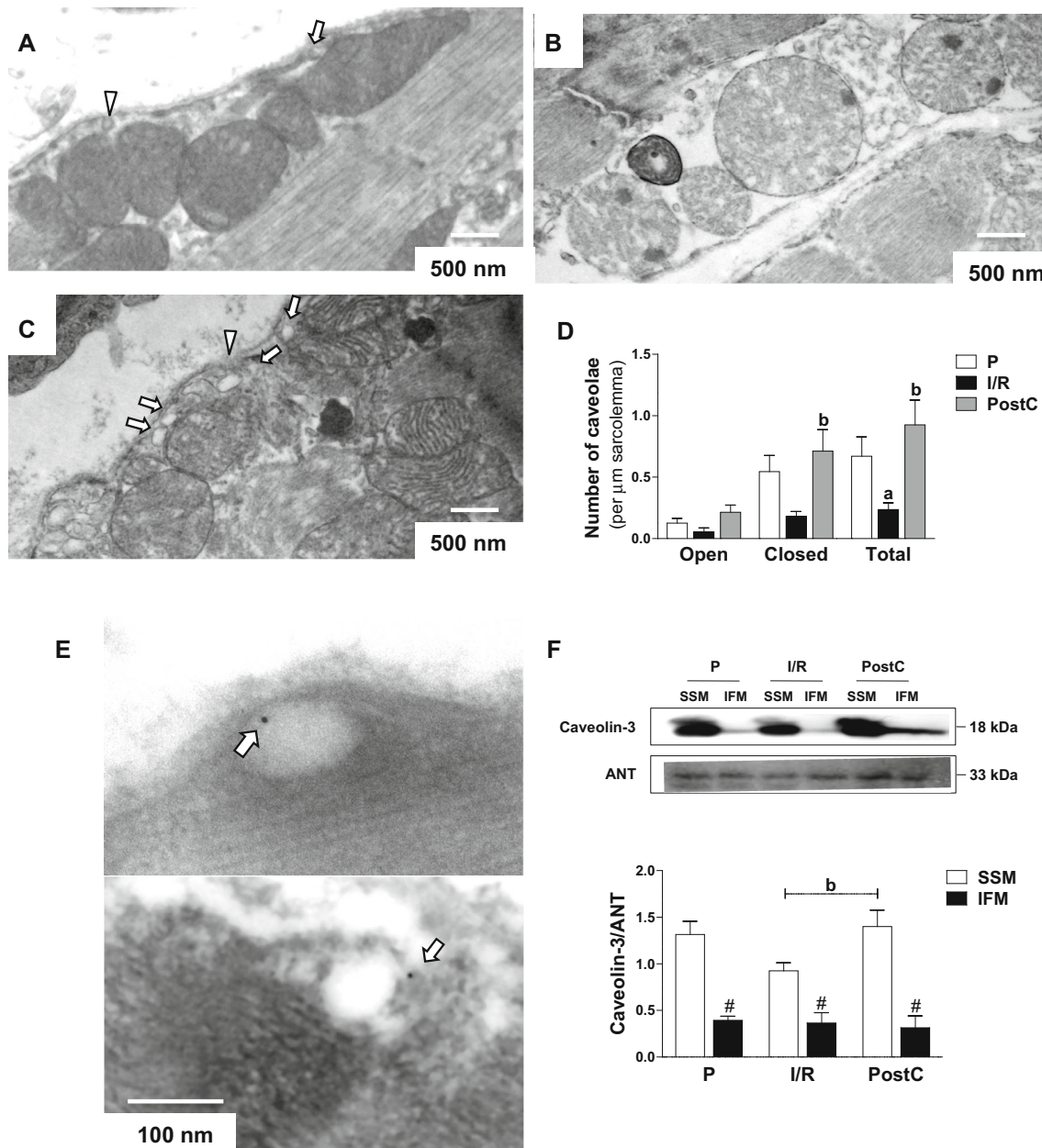


Fig. 2 Identification of caveolae interacting with mitochondria from perfused (P), ischemic-reperfused (I/R) and postconditioned hearts (PostC). Representative electron microscopy images showing the presence of caveolae integrated into the sarcolemma (*arrowheads*) or caveolar vesicles (*arrows*). **a** P group and, **b** I/R cardiomyocytes. **c** Open and closed (vesicular) caveolae observed in the PostC group. **d** Quantitative analysis of the number of open and closed caveolae along sarcolemma from all groups. Values are mean \pm SEM, $n = 25$ micrographs per group. ^a $p < 0.05$ vs. P; ^b $p < 0.05$ vs. I/R (two-way ANOVA). The main effect for group yielded an F ratio of (2,81) = 10.07, $p < 0.001$. The main effect for caveolae yielded an F ratio of (2,81) = 9.98, $p < 0.001$. The interaction effect was not

significant ($p = 0.321$). **e** Representative immunoelectron microscopy images showing the presence of caveolae and caveolin-3 labeling (12 nm particle, *arrows*) in PostC group. **f** Representative immunoblots of caveolin-3 levels in mitochondrial subpopulations and densitometric ratio between caveolin-3 and adenine nucleotide translocator (ANT). IFM interfiibrillar mitochondria. Values are mean \pm SEM, $n = 4$. ^b $p < 0.05$ vs. I/R; [#] $p < 0.05$ vs. SSM (two-way ANOVA). The main effect for mitochondrial subpopulation render an F ratio of (1,18) = 74.29, $p < 0.001$. No significance was found either in the main effect of group or in the interaction effect ($p > 0.05$)

period to deplete membrane cholesterol and disrupt caveolae (Fig. 4a). As expected, PostC-conferred cardioprotection was lost in the presence of M β CD. LVDP (Fig. 4b),

heart rate (Fig. 4c) and DP (Fig. 4d) were depressed, whereas no effect was observed in P hearts treated with M β CD. Also, infarct size increased (Fig. 4e), caveolar

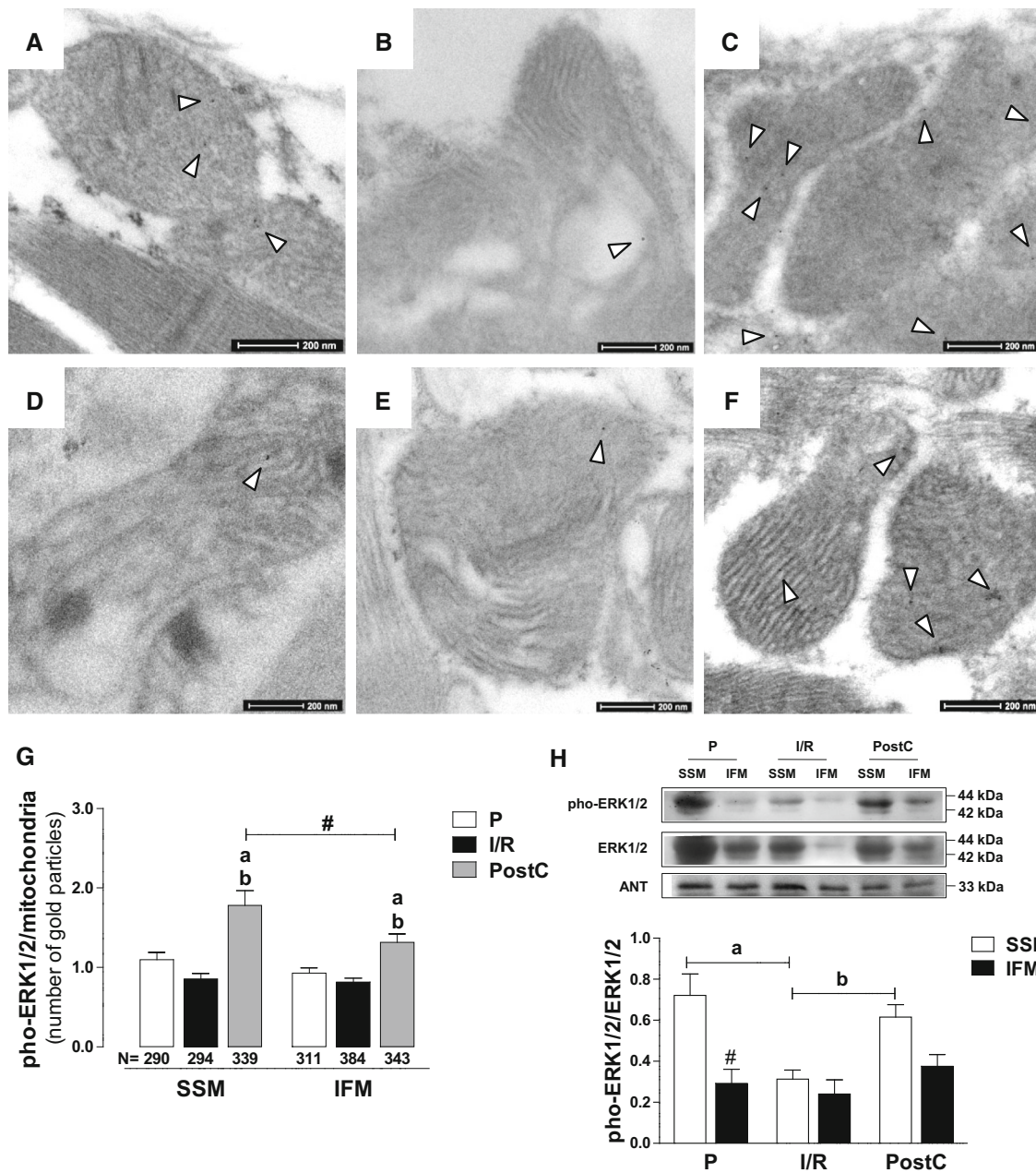


Fig. 3 PostC-induced ERK1/2 signaling to mitochondria. Representative immunoelectron microscopy images showing the presence of pho-ERK1/2 (5 nm particle, *arrowheads*) in **a** subsarcolemmal mitochondria (SSM) and **d** interfibrillar mitochondria (IFM) from P group. **b** SSM and **e** IFM subpopulations from I/R group. **c** SSM and **f** IFM from PostC. **g** Quantitative analysis of gold particles labeling pho-ERK1/2 per mitochondria. *N* number of mitochondria analyzed from micrographs obtained from five independent heart preparations for each group. Values are mean ± SEM. ^a*p* < 0.05 vs. P; ^b*p* < 0.05 vs. I/R; [#]*p* < 0.05 vs. SSM (two-way ANOVA). The main effect for group yielded a *F* ratio of (2,1576) = 26.6, *p* < 0.001 and a significant main effect for mitochondrial subpopulation, *F*(1,1576) = 6.982, *p* < 0.01.

There was no interaction between main effects (*p* = 0.114). **h** Representative immunoblots of pho-ERK1/2 in both mitochondrial subpopulations and densitometric ratio between pho-ERK1/2/total ERK1/2. ANT levels are presented as further control loading. SSM subsarcolemmal mitochondria, IFM interfibrillar mitochondria, ERK extracellular signal-regulated kinases, ANT adenine nucleotide translocator. Values are mean ± SEM. *n* = 5. ^a*p* < 0.001 vs. I/R; ^b*p* < 0.05 vs. PostC; [#]*p* < 0.05 vs. SSM (two-way ANOVA). The main effect for group yielded an *F* ratio of (2,24) = 6.82, *p* = 0.0045 and the main effect for mitochondrial subpopulation an *F* ratio of (1,24) = 20.48, *p* = 0.001. The interaction between main effects was significant (*p* = 0.0367)

microdomains were disrupted (Fig. 5a) and pho-ERK1/2 immunogold labeling decreased after MβCD treatment of PostC hearts in both SSM (Fig. 5b) and in IFM (Fig. 5c), as

the quantitative analysis showed (Fig. 5d). On the other hand, it is worth mentioning that heart performance from I/R + MβCD was lost immediately to reperfusion (data not

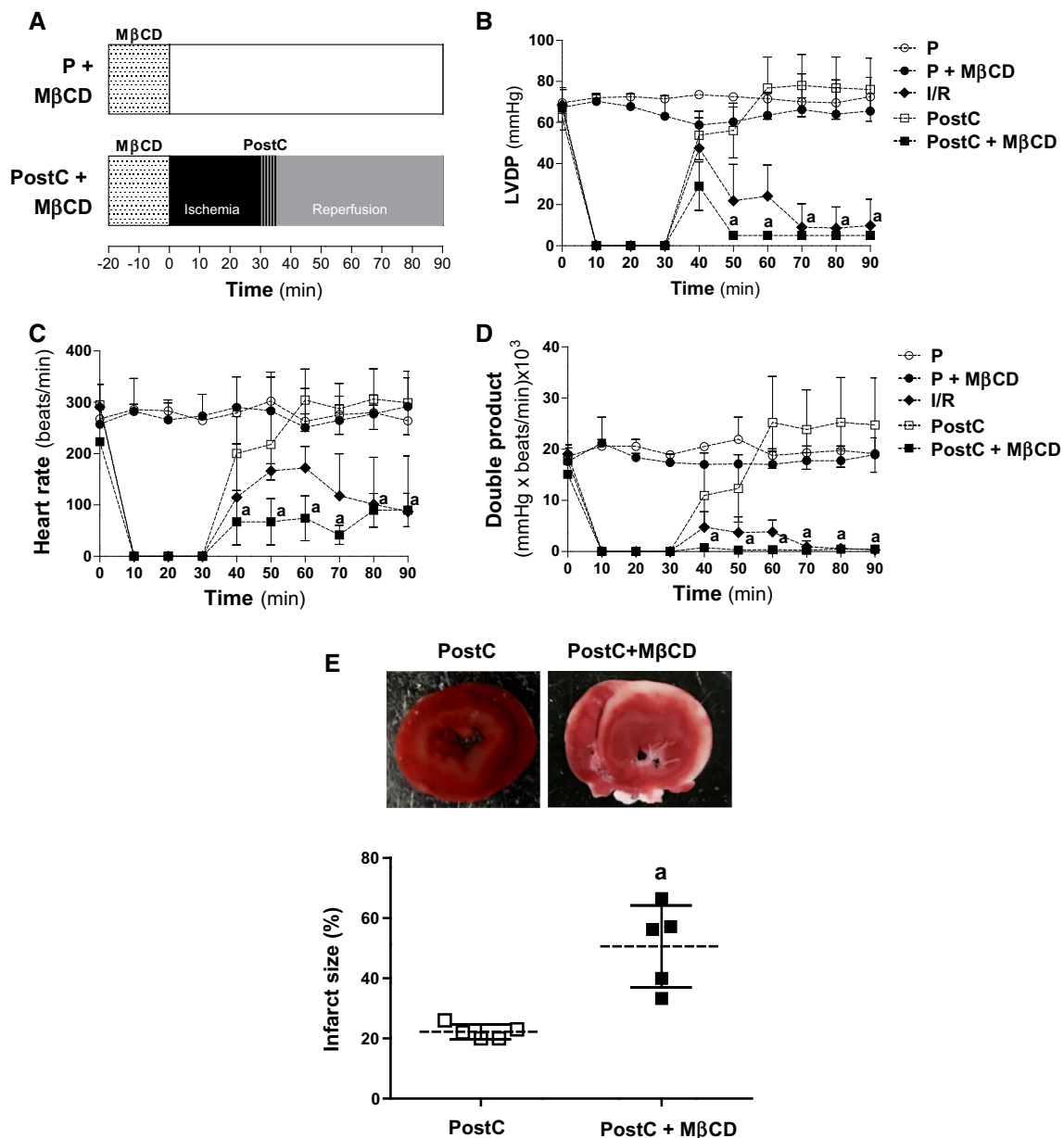


Fig. 4 M β CD abolishes PostC-induced protection in reperused hearts. **a** Schematic representation of 0.1 mM M β CD administration to perfused hearts (P + M β CD) and postconditioned hearts (PostC + M β CD). **b** Left ventricular diastolic pressure (LVDP),

c heart rate and **d** double product. Values are mean \pm SEM, $n = 6$. $^a p < 0.05$ vs. P + M β CD (one-way ANOVA). **e** Infarct size percentage and representative images of TTC-stained hearts. Values are mean \pm SEM, $n = 5$. $^a p < 0.05$ vs. PostC (paired t test)

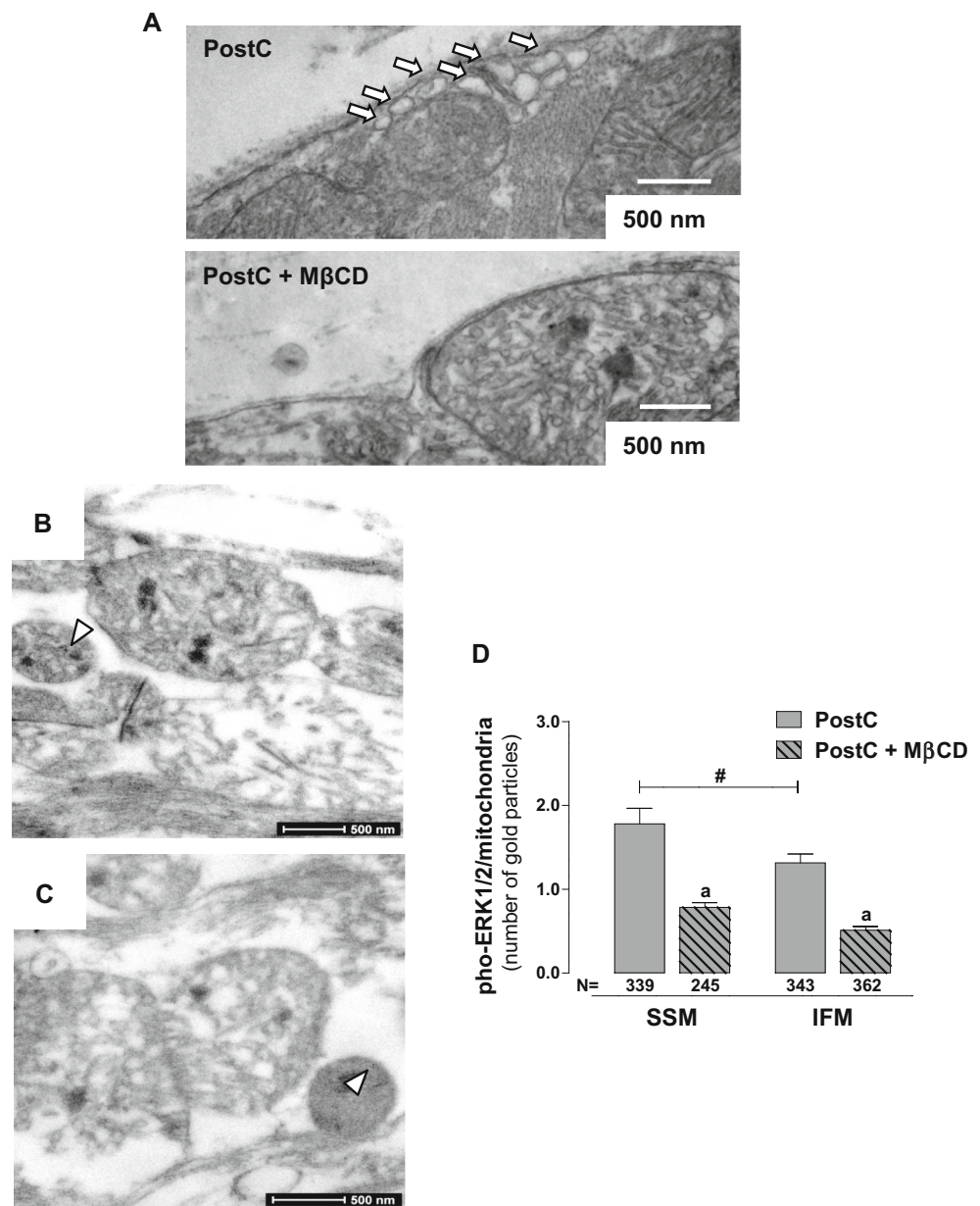
shown), therefore this group was not included in subsequent analyses.

PostC-induced inhibition of mPTP opening is abolished by M β CD in SSM and IFM

The next question was if caveolae disruption and concomitant ERK1/2 signaling inhibition were related with increased susceptibility to mPTP opening in mitochondrial subpopulations, particularly in SSM. Matrix swelling, extramitochondrial free Ca $^{2+}$ transport and $\Delta\Psi_m$ changes were

evaluated (Fig. 6). SSM and IFM from the I/R group showed significant swelling in the presence of 100 μ M Ca $^{2+}$ in comparison with P group ($p < 0.05$); although SSM swelling was approximately 30% greater than in IFM. PostC inhibited Ca $^{2+}$ -induced mPTP opening in IFM more efficiently than CsA administration in vitro and to a similar extent in SSM. This result suggests that SSM are more prone to permeability transition than IFM. However, the inhibitory effect of PostC on mPTP opening was completely abolished by M β CD treatment in both mitochondrial subpopulations (Fig. 6a, b). Accordingly, SSM and IFM from the I/R group

Fig. 5 M β CD diminishes caveolae formation and ERK1/2 activation in mitochondria from PostC hearts. **a** Representative electron microscopy images showing the effect of M β CD in caveolae formation, and **b** in pho-ERK1/2 immunogold labeling in subsarcolemmal mitochondria (SSM) and **c** interfibrillar mitochondria (IFM). **d** Quantitative analysis of gold particles labeling pho-ERK1/2 per mitochondria. *N* number of mitochondria analyzed from micrographs obtained from five independent heart preparations from each group. Values are mean \pm SEM. ^a*p* < 0.05 vs. PostC; [#]*p* < 0.05 vs. SSM (two-way ANOVA). The main effect for group yielded an *F* ratio of (1,1285) = 56.27, *p* < 0.001 and a significant main effect for mitochondrial subpopulation, *F*(1,1285) = 9.443, *p* < 0.01. There was no interaction between main effects (*p* = 0.421)



lose their capacity to transport and accumulate Ca^{2+} , although IFM retained this cation more efficiently than SSM. PostC preserves the capacity to buffer Ca^{2+} overload in both subpopulations, until the protonophore CCCP was added. Mitochondria from Post + M β CD group did not accumulate calcium (Fig. 6c, d).

The effect of substrate oxidation, ATP synthesis and calcium handling was evaluated on the maintenance of $\Delta\Psi_m$ (Fig. 6e, f; Table 1). Membrane polarization induced by the addition of substrate was partially dissipated in the presence of ADP in all conditions. When the re-entry of protons into the matrix was blocked with the F_1F_0 -ATPase inhibitor oligomycin, lower membrane repolarization was achieved in the I/R group from both mitochondrial

subpopulations (*p* < 0.05), indicating that proton leak occurs independently of Complex V. PostC and to a lesser extent CsA, successfully restored $\Delta\Psi_m$ to the values observed in mitochondria from the P group in both SSM and IFM. Transmembrane potential in mitochondria isolated from I/R hearts was collapsed in the presence of 50 μM CaCl_2 , indicating deregulation in calcium handling in both subpopulations, which was recovered in the PostC groups. CCCP-induced depolarization was less evident in SSM and IFM subpopulations from I/R in comparison with P and PostC groups (*p* < 0.05); although changes in fluorescence intensity were significantly bigger in IFM than in SSM indicating higher transmembrane potential in the former subpopulation (*p* < 0.05). Mitochondrial

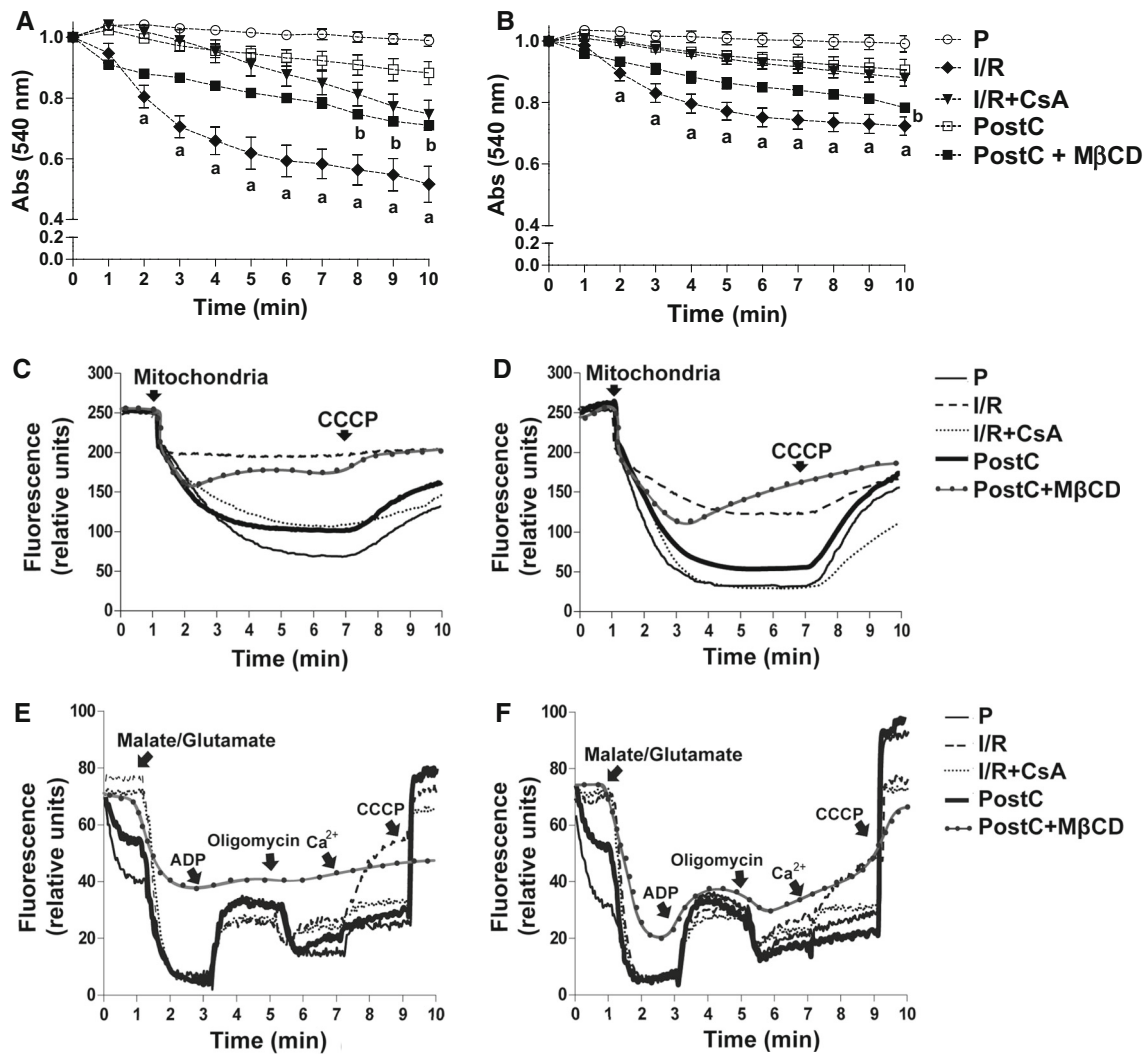


Fig. 6 Effect of M β CD on mitochondrial permeability transition pore (mPTP) opening in mitochondrial subpopulations from PostC. Mitochondrial swelling in **a** SSM and **b** IFM evaluated in the presence of 100 μ M Ca²⁺. Values are mean \pm SEM, of at least five independent experiments. ^a $p < 0.05$ vs. P; ^b $p < 0.05$ vs. PostC (two-way-ANOVA). In SSM, the main effect for group yielded an F ratio of (4,231) = 170.18, $p < 0.001$ and a significant main effect for time $F(9,231) = 26.53$ $p < 0.001$. The interaction effect was significant, $F(40,231) = 3.78$, $p < 0.001$. In IFM the main effect for group yielded an F ratio of (4,231) = 135.91, $p < 0.001$ and a significant main effect for time, $F(9,231) = 25.82$ $p < 0.001$. The interaction

effect was significant, $F(40,231) = 2.85$, $p < 0.001$. Mitochondrial Ca²⁺ retention in **c** SSM and **d** IFM subpopulations. Tracings are representative of at least three different experiments. Mitochondrial membrane potential changes ($\Delta\Psi_m$) in **e** SSM and **f** IFM subpopulations assessed by adding different substrates. Tracings are representative of at least four different experiments. SSM subsarcolemmal mitochondria, IFM interfibrillar mitochondria, CsA cyclosporine A, CCCP carbonyl cyanide *m*-chlorophenylhydrazone, RFU relative fluorescence units, P perfused hearts, I/R ischemic-reperfused hearts, PostC postconditioned hearts

subpopulations isolated from Post + M β CD group were unresponsive to substrate oxidation and CCCP addition did not exert further depolarization. In correlation with these data, mitochondrial ultrastructure showed that PostC diminished matrix swelling, cristae disruption, mitochondrial area and integrated density in both SSM and IFM observed in the I/R group and, that PostC-related preservation in mitochondrion morphology was abolished with M β CD treatment (Supplementary Figure S.4).

Relevance of SSM and IFM location in cardiac cells and their functional response in the setting of I/R and PostC

The differential susceptibility to mPTP opening observed between the mitochondrial subpopulations, motivated us to look for further functional responses related with their distribution during reperfusion and PostC. We performed oxygen consumption experiments, measured oxidative

Table 1 Effect of postconditioning on mitochondrial membrane potential ($\Delta\Psi_m$) dissipation of SSM and IFM subpopulations

	P	I/R	I/R + CsA	PostC
SSM (RFU)				
ADP-stimulated depolarization	27.7 ± 1.4	18.7 ± 1.5	19.6 ± 0.8	25.5 ± 2.7
Oligomycin-induced polarization	16.4 ± 2.4	0.7 ± 1.4 ^a	4.9 ± 1.2 ^b	11.1 ± 3.2 ^b
Ca ²⁺ -induced depolarization	8.6 ± 1.4	27.0 ± 4.8 ^a	8.9 ± 0.7 ^b	8.7 ± 1.7 ^b
CCCP-induced depolarization	57.0 ± 1.5	15.0 ± 5.4 ^a	34.6 ± 1.5 ^{a,b}	52.5 ± 5.7 ^b
IFM (RFU)				
ADP-stimulated depolarization	25.9 ± 1.5	20.2 ± 1.6	18.9 ± 1.3	24.6 ± 1.8
Oligomycin-induced polarization	14.3 ± 1.1	4.7 ± 2.5	5.0 ± 3.0	15.3 ± 1.2 ^b
Ca ²⁺ -induced depolarization	5.6 ± 2.2	22.5 ± 6.6 ^a	7.6 ± 0.3 ^b	4.3 ± 1.9 ^b
CCCP-induced depolarization	67.3 ± 4.6	36.6 ± 7.0 ^{a,#}	48.9 ± 3.0 ^{a,b}	72.0 ± 0.6 ^{b,#}

Values are mean ± SEM, $n = 4$

P perfused, I/R ischemia–reperfusion, PostC postconditioning, CsA cyclosporine A, RFU relative fluorescence units

[#] $p < 0.05$ vs. SSM (two-way ANOVA)

^a $p < 0.05$ vs. P

^b $p < 0.05$ vs. I/R

stress, the antioxidant response and cytochrome c release in both SSM and IFM.

Basal oxygen consumption (State 4) using NADH-linked substrates or succinate increased in IFM, whereas ADP-stimulated respiration (State 3) was lost in both mitochondrial subpopulations from the I/R group. As maximal uncoupled respiration was also diminished, it follows that lower RC in both mitochondria result from substrate oxidation inhibition, rather than from dysfunction in ATP synthesis. The same behavior was observed with both substrates, confirming that Complex I function and of other downstream respiratory complex are jeopardized during I/R. However, worth mentioning that lower RC values were observed in SSM than in IFM, independently of the oxidized substrate. PostC attenuated all these alterations ($p < 0.05$), although some parameters were also different to those observed in the corresponding subpopulations of the P group using malate/glutamate (RC and ADP/O ratio) or succinate (State 3, RC and ADP/O ratio) ($p < 0.05$) (Table 2).

We also evaluated the susceptibility of both subpopulations to oxidative damage occurring during I/R. Increased lipid peroxidation, as well as decreased GSH levels and aconitase activity were observed in the SSM subpopulation from the I/R group as compared to P group ($p < 0.05$) (Fig. 7). PostC reduced MDA levels by 43% (10.8 ± 0.8 to 6.1 ± 0.5 nmol MDA/mg protein) ($p < 0.05$) (Fig. 7a); maintained GSH content and preserved aconitase activity (86 and 34%, respectively) as compared with the I/R group in this subpopulation ($p < 0.05$) (Fig. 7b, c). Lipid peroxidation was about 50% lower in IFM than in SSM ($p < 0.05$) (Fig. 5a) and neither GSH levels nor aconitase activity changed between the groups ($p > 0.05$) (Fig. 7b, c).

A significant reduction in the activities of SOD, CAT, GPx and GR were observed in the SSM subpopulation from the I/R group in comparison with the P group ($p < 0.05$) (Fig. 7). PostC maintained the activity of SOD (Fig. 7d), CAT (Fig. 7e) and GPx (Fig. 7f) similar to control values ($p > 0.05$), but did not prevent decrease in GR activity (Fig. 7g). On the other hand, the activities of the evaluated antioxidant enzymes were not affected by I/R in the IFM subpopulation ($p > 0.05$) (Fig. 7d–g). In fact, GPx activity was significantly higher in IFM than in SSM subjected to either I/R (157.9 ± 4.2 U/mg protein vs. 118.3 ± 5.7 U/mg protein) or to PostC (171.7 ± 6.1 U/mg protein vs. 141.4 ± 6.9 U/mg protein) ($p < 0.05$) (Fig. 7f).

Finally, we determined that Ca²⁺ overload promoted major cyt c release in SSM ($p < 0.05$) than in IFM from the I/R group, as compared with the P group ($p > 0.05$). PostC prevented effectively from cyt c release in both subpopulations ($p < 0.05$), whereas CsA only exerted a partial protection (Supplementary Figure S.5).

Discussion

In this study, we demonstrated that cardioprotective ERK1/2 signaling is directed to mitochondria through caveolae/signalosomes in isolated perfused hearts subjected to PostC. We observed for the first time, that PostC increases the number of caveolae along sarcolemma in close association with augmented ERK1/2 activation in SSM and in IFM, supporting data from other groups that described the association between caveolae and mitochondria in cardiac myocytes subjected to ischemic preconditioning (IPC) [31] and in targeted-gene transfer of

Table 2 Effect of postconditioning on SSM and IFM oxygen consumption using malate/glutamate or succinate as substrates

	Subsarcolemmal mitochondria (SSM)			Interfibrillar mitochondria (IFM)		
	P	I/R	PostC	P	I/R	PostC
Malate/glutamate						
State 4 (ngAtO/mg/min)	42.1 ± 2.5	34.1 ± 6.2	43.4 ± 2.8	38.4 ± 4.2	50.8 ± 5.1 [#]	50.8 ± 3.4
State 3 (ngAtO/mg/min)	121.4 ± 6.0	42.7 ± 10.1 ^a	94.8 ± 5.0 ^b	165.3 ± 13.1 [#]	83.6 ± 6.0 ^{a,#}	142.4 ± 5.0 ^{b,#}
RC	2.9 ± 0.1	1.2 ± 0.1 ^a	2.3 ± 0.2 ^{a,b}	4.4 ± 0.2 [#]	1.7 ± 0.1 ^a	2.9 ± 0.2 ^{a,b}
Uncoupled respiration (ngAtO/mg/min)	135.0 ± 22.5	37.8 ± 9.9 ^a	111.5 ± 15.4 ^b	170.3 ± 28.6	87.3 ± 10.2 ^a	161.6 ± 6.3 ^b
ADP/O ratio	2.3 ± 0.1	1.3 ± 0.1 ^a	1.7 ± 0.1 ^{a,b}	2.6 ± 0.1	1.6 ± 0.1 ^a	2.0 ± 0.1 ^{a,b}
Succinate						
State 4 (ngAtO/mg/min)	66.3 ± 6.9	60.7 ± 11.0	65.0 ± 5.8	72.5 ± 2.9	91.0 ± 7.3 [#]	83.0 ± 4.7
State 3 (ngAtO/mg/min)	166.0 ± 10.7	67.5 ± 13.0 ^a	125.1 ± 11.4 ^{a,b}	224.2 ± 10.0 [#]	135.6 ± 10.9 ^{a,#}	182.1 ± 6.0 ^{a,b,#}
RC	2.6 ± 0.1	1.1 ± 0.1 ^a	2.0 ± 0.1 ^{a,b}	3.1 ± 0.2 [#]	1.5 ± 0.1 ^a	2.2 ± 0.1 ^{a,b}
Uncoupled respiration (ngAtO/mg/min)	160.4 ± 19.5	74.3 ± 16.4 ^a	137.5 ± 11.6 ^b	226.0 ± 10.5 [#]	143.7 ± 17.5 ^{a,#}	197.6 ± 6.9 ^{b,#}
ADP/O ratio	2.2 ± 0.1	1.1 ± 0.1 ^a	1.7 ± 0.1 ^{a,b}	2.4 ± 0.1	1.4 ± 0.1 ^a	1.9 ± 0.1 ^{a,b}

Values are mean ± SEM, $n = 7$

P perfused, I/R ischemia–reperfusion, PostC postconditioning, RC respiratory control

[#] $p < 0.05$ vs. SSM (two-way ANOVA)

^a $p < 0.05$ vs. P

^b $p < 0.05$ vs. I/R

caveolin to mitochondria [15]. Preferential targeting of these kinases towards SSM might be due to the proximity of caveolae with sarcolemmal membrane; although internalized caveolae near IFM have also been observed in cardiomyocytes from mice exposed to isoflurane [40]. Other caveolae-associated signaling proteins include PKC isoforms, Akt and GSK3 β [21, 33, 37], which confirm multiple signaling pathways from the plasma membrane to internal compartments, as indicated by the increase in endothelial nitric oxide synthase (eNOS) and caveolin-3 levels in SSM from preconditioned hearts [37]. The finding that PostC-induced ERK1/2 activation in mitochondria occurs mainly in fractions containing intermembrane space proteins and to minor extent in the outer membrane fraction, led us to propose that cytosolic pho-ERK1/2 interacts transiently with outer membrane phosphorylating mitochondrial targets, which in turn activates a mitochondrial ERK1/2 pool. Other groups have reported that pho-ERK1/2 increased in fractions composed of both outer membrane and intermembrane space in rat brain under developmental modulation [2]. Also, the existence of a mitochondrial ERK1/2 pool, which depends on cytosolic ERK activation has been described [16] and furthermore, that mitochondrial ERK1/2 might be activated by PKC ϵ in the same compartment [3]. This hypothesis could explain ERK1/2 regulation of diverse mitochondrial targets and processes, e.g., the mitochondrial permeability transition pore [45], oxidative phosphorylation proteins [29], ROS

production [24], cholesterol transport [12], autophagy [44] and mitochondrial fission [39].

On the other hand, the analysis of SSM and IFM function confirmed that damage in SSM was greater than in IFM during reperfusion. Mitochondrial respiration was recovered in both subpopulations, although responsiveness to cardioprotective signaling of the two distinct types of mitochondrial subpopulations was based on this sensitivity [26, 27]. This result contrasted with an earlier report in which mitochondrial respiration was not recovered either in SSM or in IFM in PostC [30]. This inconsistency might be explained in basis of the different experimental setting and model used by that group.

Further evidence of the protection afforded by PostC in both mitochondrial subpopulations was observed after measuring oxidative stress markers. Our results demonstrate that SSM is more affected by I/R-induced damage, as this subpopulation is exposed to higher oxygen levels than the IFM [26]. In a similar way, SSM from I/R hearts exhibited a deficient antioxidant system, while the enzymatic activity in IFM was not affected. PostC improved the antioxidant response in SSM subpopulation, making sense with the proposal that the location of mitochondria define their role within the cell [26]. Increased resistance of IFM to calcium overload might result from nearness to the sarcoplasmic reticulum and their continuous exposition to calcium oscillations during the contraction–relaxation cycle [34]. As cyt c release and apoptosis triggering has been related with Ca²⁺-

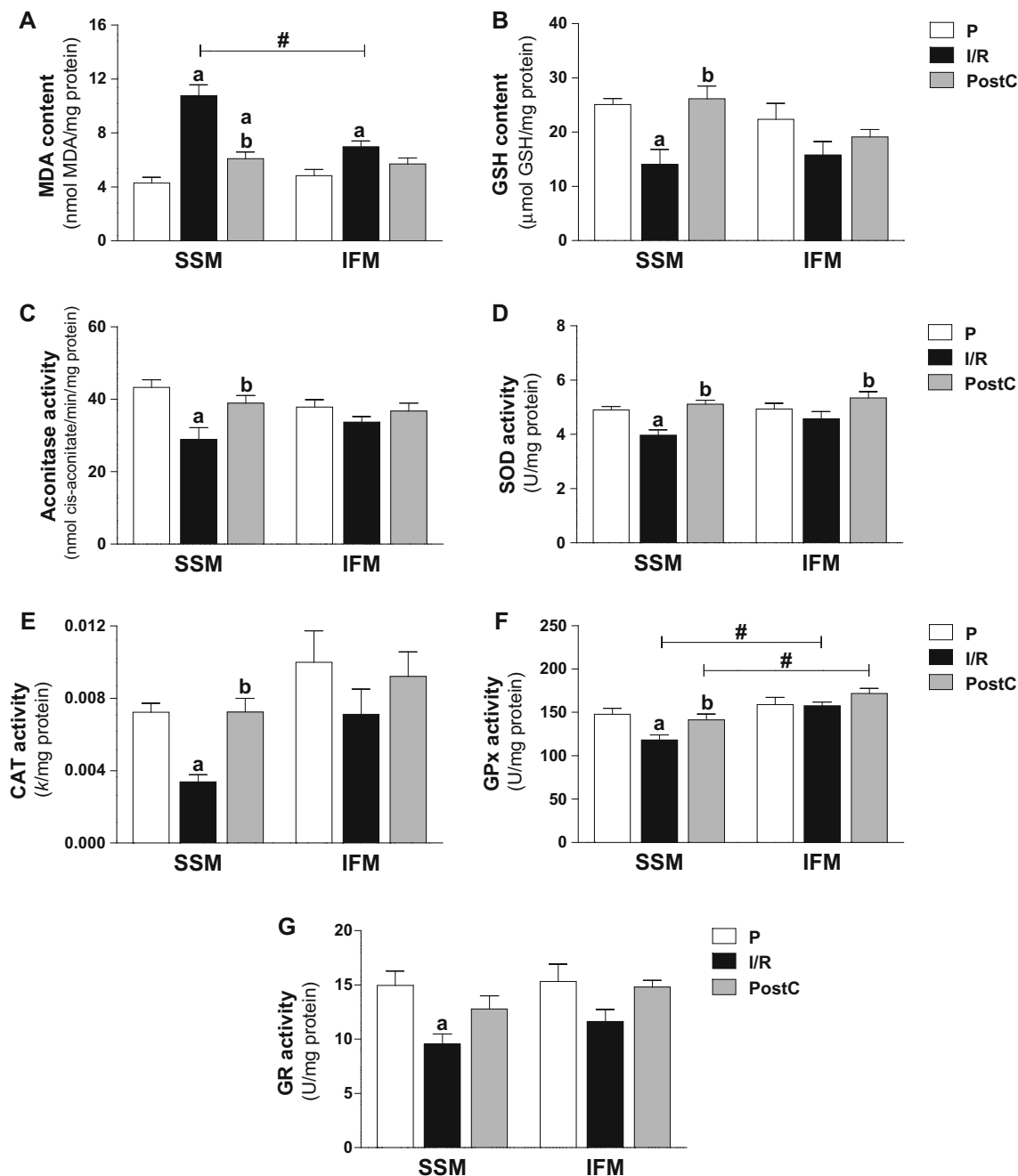


Fig. 7 Oxidative stress markers and antioxidant enzyme activities in mitochondrial subpopulations isolated from perfused hearts (P), ischemic-reperfused hearts (I/R) and postconditioned hearts (PostC). **a** MDA content, **b** GSH content, **c** aconitase, **d** SOD, **e** CAT, **f** GPx and **g** GR activities. *SSM* subsarcolemmal mitochondria, *IFM*

interfibrillar mitochondria, *MDA* malondialdehyde, *GSH* glutathione, *SOD* superoxide dismutase, *CAT* catalase, *GPx* glutathione peroxidase, *GR* glutathione reductase. Values are mean ± SEM, *n* = 6. ^a*p* < 0.05 vs. P; ^b*p* < 0.05 vs. I/R; #*p* < 0.05 vs. SSM (two-way ANOVA)

induced increase in membrane permeability, the resistance to calcium overload of IFM [7] might explain why this subpopulation retained *cyt c* more efficiently than SSM. Other possibility is that the lower levels of cardiolipin measured in SSM but not in IFM after ischemia in rabbit [27] might account for reduction in the respiration rate, as well as for augmented cytochrome *c* release in SSM.

The above data, along with the recent demonstration that caveolin-3 overexpression in mice concurs with decreased heart rate and augmented ion channel expression [36], highlight the diversity of processes involved in caveolin signaling and brings to the forefront the emerging interactions between caveolins and new signaling proteins [42].

Conclusion

Overall, our results suggest that ERK1/2 signaling through caveolae interaction with SSM is more productive to overall cardiac function than signaling delivered to IFM. We propose that ERK1/2 is activated and recruited into caveolae during PostC, interacting with cardiac mitochondrial subpopulations. By this mechanism, the highly susceptible SSM subpopulation maintains respiratory activity and becomes resistant to oxidative stress and to mitochondrial permeability transition pore opening. Future investigations are needed to determine how caveolae migrate from the sarcolemma to the mitochondria and to identify new mitochondrial targets for PostC-induced kinase regulation.

Acknowledgements The authors thank Rocio Torrico-Lavayen for technical assistance.

Compliance with ethical standards

Conflict of interest The authors declare that they have no conflict of interest.

Ethical standard All authors in this work gave their informed consent prior to their inclusion in the study. The manuscript does not contain clinical studies or patient data.

Funding This work was supported by Grant 177527 to CZ, 181593 to FC and 220046 to JP-Ch from the National Council of Science and Technology (CONACYT), Mexico.

References

- Aldakkak M, Stowe DF, Dash RK, Camara AKS (2013) Mitochondrial handling of excess Ca^{2+} is substrate-dependent with implications for reactive oxygen species generation. *Free Radic Biol Med* 56:193–203. doi:[10.1016/j.freeradbiomed.2012.09.020](https://doi.org/10.1016/j.freeradbiomed.2012.09.020)
- Alonso M, Melani M, Converso D, Jaitovich A, Paz C, Carreras MC, Medina JH, Poderoso JJ (2004) Mitochondrial extracellular signal-regulated kinases 1/2 (ERK1/2) are modulated during brain development. *J Neurochem* 89:248–256. doi:[10.1111/j.1471-4159.2004.02323.x](https://doi.org/10.1111/j.1471-4159.2004.02323.x)
- Baines CP, Zhang J, Wang GW, Zheng YT, Xiu JX, Cardwell EM, Bolli R, Ping P (2002) Mitochondrial PKCepsilon and MAPK form signaling modules in the murine heart: enhanced mitochondrial PKCepsilon-MAPK interactions and differential MAPK activation in PKCepsilon-induced cardioprotection. *Circ Res* 90:390–397. doi:[10.1161/01.RES.0000069215.36389.8D](https://doi.org/10.1161/01.RES.0000069215.36389.8D)
- Boengler K, Stahlhofen S, Sand A, Gres P, Ruiz-Meana M, García-Dorado D, Heusch G, Schulz R (2009) Presence of connexin 43 in subsarcolemmal, but not in interfibrillar cardiomyocyte mitochondria. *Basic Res Cardiol* 104:141–147. doi:[10.1007/s00395-009-0007-5](https://doi.org/10.1007/s00395-009-0007-5)
- Chang G, Zhang D, Yu H, Zhang P, Wang Y, Zheng A, Qin S (2013) Cardioprotective effects of exenatide against oxidative stress-induced injury. *Int J Mol Med* 32:1011–1020. doi:[10.3892/ijmm.2013.1475](https://doi.org/10.3892/ijmm.2013.1475)
- Chávez E, Briones R, Michel B, Bravo C, Jay D (1985) Evidence for the involvement of dithiol groups in mitochondrial calcium transport: studies with cadmium. *Arch Biochem Biophys* 242:493–497. doi:[10.1016/0003-9861\(85\)90235-8](https://doi.org/10.1016/0003-9861(85)90235-8)
- Chen Q, Ross T, Hu Y, Lesnefsky EJ (2012) Blockade of electron transport at the onset of reperfusion decreases cardiac injury in aged hearts by protecting the inner mitochondrial membrane. *J Aging Res* 2012:753949. doi:[10.1155/2012/753949](https://doi.org/10.1155/2012/753949)
- Correa F, García N, Gallardo-Pérez J, Carreño-Fuentes L, Rodríguez-Enríquez S, Marín-Hernández A, Zazueta C (2008) Post-conditioning preserves glycolytic ATP during early reperfusion: a survival mechanism for the reperfused heart. *Cell Physiol Biochem* 22:635–644. doi:[10.1159/000185547](https://doi.org/10.1159/000185547)
- Correa F, García N, Robles C, Martínez-Abundis E, Zazueta C (2008) Relationship between oxidative stress and mitochondrial function in the post-conditioned heart. *J Bioenerg Biomembr* 40:599–606. doi:[10.1007/s10863-008-9186-2](https://doi.org/10.1007/s10863-008-9186-2)
- Correa F, Zazueta C (2005) Mitochondrial glycosidic residues contribute to the interaction between ruthenium amine complexes and the calcium uniporter. *Mol Cell Biochem* 272:55–62. doi:[10.1007/s11010-005-6754-1](https://doi.org/10.1007/s11010-005-6754-1)
- Kalogeris T, Baines CP, Krenz M, Korthuis RJ (2012) Cell biology of ischemia/reperfusion injury. *Int Rev Cell Mol Biol* 298:229–317. doi:[10.1016/B978-0-12-394309-5.00006-7](https://doi.org/10.1016/B978-0-12-394309-5.00006-7)
- Duarte A, Castillo AF, Podestá EJ, Poderoso C (2014) Mitochondrial fusion and ERK activity regulate steroidogenic acute regulatory protein localization in mitochondria. *PLoS One* 9:e100387. doi:[10.1371/journal.pone.0100387](https://doi.org/10.1371/journal.pone.0100387)
- Fernandez-Gomez FJ, Galindo MF, Gomez-Lazaro M, González-García C, Cēna V, Aguirre N, Jordán J (2005) Involvement of mitochondrial potential and calcium buffering capacity in minocycline cytoprotective actions. *Neuroscience* 133:959–967. doi:[10.1016/j.neuroscience.2005.03.019](https://doi.org/10.1016/j.neuroscience.2005.03.019)
- Folino A, Sprio AE, Di Scipio F, Berta GN, Rastaldo R (2015) Alpha-linolenic acid protects against cardiac injury and remodeling induced by beta-adrenergic overstimulation. *Food Funct* 6:2231–2239. doi:[10.1039/c5fo00034c](https://doi.org/10.1039/c5fo00034c)
- Fridolfsson HN, Kawaraguchi Y, Ali SS, Panneerselvam M, Niesman IR, Finley JC, Kellerhals SE, Migita MY, Okada H, Moreno AL, Jennings M, Kidd MW, Bonds JA, Balijepalli RC, Ross RS, Patel PM, Miyanochara A, Chen Q, Lesnefsky EJ, Head BP, Roth DM, Insel PA, Patel HH (2012) Mitochondria-localized caveolin in adaptation to cellular stress and injury. *FASEB J* 26:4637–4649. doi:[10.1096/fj.12-215798](https://doi.org/10.1096/fj.12-215798)
- Galli S, Jahn O, Hitt R, Hesse D, Opitz L, Plessmann U, Urlaub H, Poderoso JJ, Jares-Erijman EA, Jovin TM (2009) A new paradigm for MAPK: structural interactions of hERK1 with mitochondria in HeLa cells 4:7541. doi:[10.1371/journal.pone.0007541](https://doi.org/10.1371/journal.pone.0007541)
- García N, Zazueta C, Martínez-Abundis E, Pavón N, Chávez E (2009) Cyclosporin A is unable to inhibit carboxyatractyloside-induced permeability transition in aged mitochondria. *Comp Biochem Physiol C Toxicol Pharmacol* 149:374–381. doi:[10.1016/j.cbpc.2008.09.006](https://doi.org/10.1016/j.cbpc.2008.09.006)
- García-Niño WR, Tapia E, Zazueta C, Zatarain-Barrón ZL, Hernández-Pando R, Vega-García CC, Pedraza-Chaverrí J (2013) Curcumin pretreatment prevents potassium dichromate-induced hepatotoxicity, oxidative stress, decreased respiratory complex I activity, and membrane permeability transition pore opening. *Evid Based Complement Altern Med* 2013:424692. doi:[10.1155/2013/424692](https://doi.org/10.1155/2013/424692)
- Graziani A, Bricko V, Carmignani M, Graier WF, Groschner K (2004) Cholesterol- and caveolin-rich membrane domains are essential for phospholipase A 2-dependent EDHF formation. *Cardiovasc Res* 64:234–242. doi:[10.1016/j.cardiores.2004.06.026](https://doi.org/10.1016/j.cardiores.2004.06.026)

20. Hernández-Reséndiz S, Roldán FJ, Correa F, Martínez-Abundis E, Osorio-Valencia G, Ruíz-De-Jesús O, Alexánder-Rosas E, Viguera RM, Franco M, Zazueta C (2013) Postconditioning protects against reperfusion injury in hypertensive dilated cardiomyopathy by activating MEK/ERK1/2 signaling. *J Card Fail* 19:135–146. doi:[10.1016/j.cardfail.2013.01.003](https://doi.org/10.1016/j.cardfail.2013.01.003)
21. Hernández-Reséndiz S, Zazueta C (2014) PHO-ERK1/2 interaction with mitochondria regulates the permeability transition pore in cardioprotective signaling. *Life Sci* 108:13–21. doi:[10.1016/j.lfs.2014.04.037](https://doi.org/10.1016/j.lfs.2014.04.037)
22. Heusch G (2015) Molecular basis of cardioprotection: signal transduction in ischemic pre-, post-, and remote conditioning. *Circ Res* 116:674–699. doi:[10.1161/CIRCRESAHA.116.305348](https://doi.org/10.1161/CIRCRESAHA.116.305348)
23. Horikawa YT, Patel HH, Tsutsumi YM, Jennings MM, Kidd WK, Hagiwara Y, Ishikawa Y, Insel PA, Roth DM (2008) Caveolin-3 expression and caveolae are required for isoflurane-induced cardiac protection from hypoxia and ischemia/reperfusion injury. *J Mol Cell Cardiol* 44:123–130. doi:[10.1016/j.yjmcc.2007.10.003](https://doi.org/10.1016/j.yjmcc.2007.10.003)
24. Kulich SM, Horbinski C, Patel M, Chu CT (2007) 6-hydroxydopamine induces mitochondrial ERK activation. *Free Radic Biol Med* 43:372–383. doi:[10.1016/j.biotechadv.2011.08.021](https://doi.org/10.1016/j.biotechadv.2011.08.021)
25. Kurian GA, Berenshtein E, Saada A, Chevion M (2012) Rat cardiac mitochondrial sub-populations show distinct features of oxidative phosphorylation during ischemia, reperfusion and ischemic preconditioning. *Cell Physiol Biochem* 30:83–94. doi:[10.1159/000339043](https://doi.org/10.1159/000339043)
26. Kuznetsov AV, Margreiter R (2009) Heterogeneity of mitochondria and mitochondrial function within cells as another level of mitochondrial complexity. *Int J Mol Sci* 10:1911–1929. doi:[10.3390/ijms10041911](https://doi.org/10.3390/ijms10041911)
27. Lesnefsky EJ, Chen Q, Slabe TJ, Stoll MS, Minkler PE, Hassan MO, Tandler Bernard, Hoppel CL (2007) Ischemia, rather than reperfusion, inhibits respiration through cytochrome oxidase in the isolated, perfused rabbit heart: role of cardiolipin. *Am J Physiol Heart Circ Physiol* 287:H258–H267. doi:[10.1152/ajpheart.00348.2003](https://doi.org/10.1152/ajpheart.00348.2003)
28. Lowry O, Rosebrough N, Farr A, Randall R (1951) Protein measurement with the folin phenol reagent. *J Biol Chem* 193:265–275
29. Monick MM, Powers LS, Barrett CW, Hinde S, Ashare A, Groskreutz DJ, Nyunoya T, Coleman M, Spitz DR, Hunninghake GW (2008) Constitutive ERK MAPK activity regulates macrophage ATP production and mitochondrial integrity. *J Immunol* 180:7485–7496. doi:[10.4049/jimmunol.180.11.7485](https://doi.org/10.4049/jimmunol.180.11.7485)
30. Paillard M, Gomez L, Augeul L, Loufouat J, Lesnefsky EJ, Ovize M (2009) Postconditioning inhibits mPTP opening independent of oxidative phosphorylation and membrane potential. *J Mol Cell Cardiol* 46:902–909. doi:[10.1016/j.yjmcc.2009.02.017](https://doi.org/10.1016/j.yjmcc.2009.02.017)
31. Patel HH, Tsutsumi YM, Head BP, Niesman IR, Jennings M, Horikawa Y, Huang D, Moreno AL, Patel PM, Insel PA, Roth DM (2007) Mechanisms of cardiac protection from ischemia/reperfusion injury: a role for caveolae and caveolin-1. *FASEB J* 21:1565–1574. doi:[10.1096/fj.06-7719com](https://doi.org/10.1096/fj.06-7719com)
32. Penna C, Perrelli MG, Tullio F, Angotti C, Camporeale A, Poli V, Pagliaro P (2013) Diazoxide postconditioning induces mitochondrial protein S-Nitrosylation and a redox-sensitive mitochondrial phosphorylation/translocation of RISK elements: no role for SAFE. *Basic Res Cardiol* 108:371. doi:[10.1007/s00395-013-0371-z](https://doi.org/10.1007/s00395-013-0371-z)
33. Quinlan CL, Costa ADT, Costa CL, Pierre SV, Dos Santos P, Garlid KD (2008) Conditioning the heart induces formation of signalosomes that interact with mitochondria to open mitoKATP channels. *Am J Physiol Heart Circ Physiol* 295:H953–H961. doi:[10.1152/ajpheart.00520.2008](https://doi.org/10.1152/ajpheart.00520.2008)
34. Ruiz-Meana M, Fernandez-Sanz C, Garcia-Dorado D (2010) The SR-mitochondria interaction: a new player in cardiac pathophysiology. *Cardiovasc Res* 88:30–39. doi:[10.1093/cvr/cvq225](https://doi.org/10.1093/cvr/cvq225)
35. See Hoe LE, Schilling JM, Tarbit E, Kiessling CJ, Busija AR, Niesman IR, Du Toit E, Ashton KJ, Roth DM, Headrick JP, Patel HH, Peart JN (2014) Sarcolemmal cholesterol and caveolin-3 dependence of cardiac function, ischemic tolerance, and opioid-dergic cardioprotection. *Am J Physiol Heart Circ Physiol* 307:H895–H903. doi:[10.1152/ajpheart.00081.2014](https://doi.org/10.1152/ajpheart.00081.2014)
36. Schilling JM, Horikawa YT, Zemljic-Harpf AE, Vincent KP, Tyan L, Yu JK, McCulloch AD, Balijepalli RC, Patel HH, Roth DM (2016) Electrophysiology and metabolism of caveolin-3-overexpressing mice. *Basic Res Cardiol* 111:28. doi:[10.1007/s00395-016-0542-9](https://doi.org/10.1007/s00395-016-0542-9)
37. Sun J, Nguyen T, Aponte AM, Menazza S, Kohr MJ, Roth DM, Patel HH, Murphy E, Steenbergen C (2015) Ischemic preconditioning preferentially increases protein S-nitrosylation in sub-sarcolemmal mitochondria. *Cardiovasc Res* 106:227–236. doi:[10.1093/cvr/cvv044](https://doi.org/10.1093/cvr/cvv044)
38. Tsutsumi YM, Tsutsumi R, Hamaguchi E, Sakai Y, Kasai A, Ishikawa Y, Yokoyama U, Tanaka K (2014) Exendin-4 ameliorates cardiac ischemia/reperfusion injury via caveolae and caveolins-3. *Cardiovasc Diabetol* 13:132. doi:[10.1186/s12933-014-0132-9](https://doi.org/10.1186/s12933-014-0132-9)
39. Villalta JI, Galli S, Iacaruso MF, Arciuch VGA, Poderoso JJ, Jares-Erijman EA, Pietrasanta LI (2011) New algorithm to determine true colocalization in combination with image restoration and time-lapse confocal microscopy to map Kinases in mitochondria. *PLoS One* 6:e19031. doi:[10.1371/journal.pone.0019031](https://doi.org/10.1371/journal.pone.0019031)
40. Wang J, Schilling JM, Niesman IR, Headrick JP, Finley JC, Kwan E, Patel PM, Head BP, Roth DM, Yue Y, Patel HH (2014) Cardioprotective trafficking of caveolin to mitochondria is G-protein dependent. *Anesthesiology* 121:538–548. doi:[10.1097/ALN.0000000000000295](https://doi.org/10.1097/ALN.0000000000000295)
41. Wortzel I, Seger R (2011) The ERK cascade: distinct functions within various subcellular organelles. *Genes Cancer* 2:195–209. doi:[10.1177/1947601911407328](https://doi.org/10.1177/1947601911407328)
42. Yang Y, Ma Z, Hu W, Wang D, Jiang S, Fan C, Di S, Sun Y (2016) Yi W (2016) Caveolin-1/-3: therapeutic targets for myocardial ischemia/reperfusion injury. *Basic Res Cardiol* 111:45. doi:[10.1007/s00395-016-0561-6](https://doi.org/10.1007/s00395-016-0561-6)
43. Yu H, Yang Z, Pan S, Yang Y, Tian J, Wang L, Sun W (2015) Hypoxic preconditioning promotes the translocation of protein kinase C ϵ binding with caveolin-3 at cell membrane not mitochondrial in rat heart. *Cell Cycle* 14:3557–3565. doi:[10.1080/15384101.2015.1084446](https://doi.org/10.1080/15384101.2015.1084446)
44. Zhu J-H, Guo F, Shelburne J, Watkins S, Chu CT (2003) Localization of phosphorylated ERK/MAP kinases to mitochondria and autophagosomes in Lewy body diseases. *Brain Pathol* 13:473–481. doi:[10.1016/j.bbi.2008.05.010](https://doi.org/10.1016/j.bbi.2008.05.010)
45. Zhuang S, Kinsey GR, Yan Y, Han J, Schnellmann RG (2008) Extracellular signal-regulated kinase activation mediates mitochondrial dysfunction and necrosis induced by hydrogen peroxide in renal proximal tubular cells. *J Pharmacol Exp Ther* 325:732–740. doi:[10.1124/jpet.108.136358](https://doi.org/10.1124/jpet.108.136358)